



# ANALYSIS ON A LEARNED OFDM RECEIVER BASED PILOT-AIDED FRAME SYNCHRONIZATION BY USING DEEP PROBABILITY NEURAL NETWORKS

<sup>1</sup>SNEHALATHA KATHA, <sup>2</sup>MOHAN DAS TALARI

<sup>1</sup>Assistant professor (c), for ECE Deparement, Jntuh college of engineering Sultanpur

<sup>2</sup>Assistant professor (c), for ECE Deparement, Jntuh college of engineering Sultanpur

## ABSTRACT

This paper is designed to retrieve bits from OF DMT time-domains, without the use of explicit DFT/IDFT. Deep and complex DCCN network is developed. Both the frame sync and the PAPR (peak to average power ratio) reductions in a single pilot sequence are achieved in this study. The two systems considered are DCO-OFDM and O-FDM divided by the asymmetric based optical orthogonal frequency division (ACO-OFDM). Only strange indexed subcontractors can have the pilot symbol. The pilot signal from the receiver uses the pilot frame to detect the mirror symmetry of the pilot symbol from the synchronization algorithm. In order to optimize and approximate LMMSE and traditional CP enhancements, the DCCN receiver can exceed legacy channel estimates with varying delays and mobility on Rayleigh's fading channels. However, the proposed approach is currently not supported by popular deep learning platforms, which benefit from complex neural networks' expressive nature.

**Key words:** Pilot, OFDM, Receiver, Channel, Neural Network.

## 1. INTRODUCTION

Deep learning (DL) has recently been highlighted by its major success in computer vision(CV) (NLP). For two reasons, DL applications in different fields are encouraged. DL algorithms are firstly datadriven, thus making them more robust for imperfections in real-world systems. Secondly, the computer complexity of the DL-based algorithms involves only several levels of simple operation, for

example multiplication by matrix vectors. DL-based algorithms are much more effective when massively parallel processing architectures (eg., graphical processing units (GPUs)) are rapidly being developed, as well as in specialised chips, etc.) to be highly paralleled on competitor architectures. DL has been incorporated into the physical level and has achieved superior performance due to these advantages on several issues.

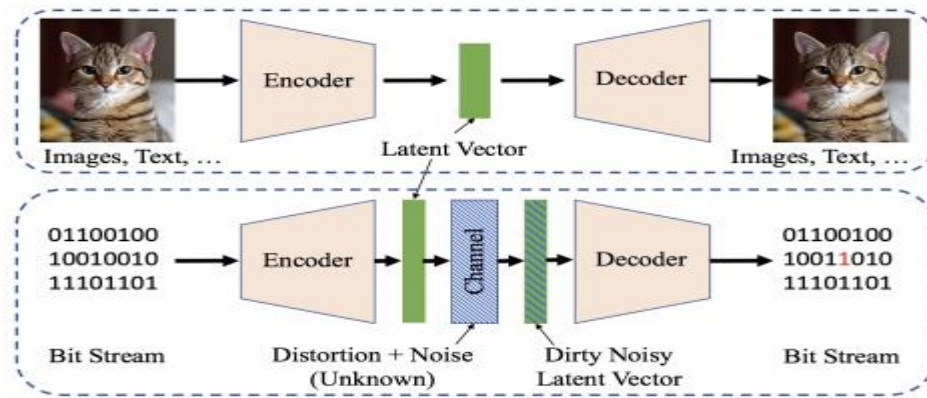


Fig. 1. General AutoEncoder (Top) v.s. Communication AutoEncoder.

A number of new tasks have been studied for deep physical (PHY) learning for wireless communications [1] – [3], including signal classification [4], [5], parameters calculation [5]-[9], the modulation channel design channel estimate design [7], and the pilot design. Deep Neural Networks (DNNs) can not only improve certain functions and wireless PHY components, but also develop a completely new communication architecture that is considered an autoencoder (AE).

The present article presents the technology of PA O-OFDM Frame Sync. The framework PAO-OFDM consists of data and pilot symbols containing asymmetric information with U-complex data signs (O-OFDM, O-OFDM, DCO-OFDM, O-OFDM, ACO-OFDM). However, only unusual indexed subcontractors have the Random Pilot Sequence, even if an Indexed Subcontractor is set at zero in both regimes. We suggest that the starting point for O-OFDM is determined using the pilot time field symmetry and the difference between the average O-OFDM symbolic strength. To compute the beginning of the PA O-OFDM frame. Each frame is a Pilot symbol as symbol times must be monitored regularly to ensure synchronisation between the transmitter and the receptor. The synchronisation algorithm has little complexity and does not require previous information about the pilot symbol sent to the receiver. Compared with the modified PO-sync approach[5,9], our proposed PA-synchronizing system also has a relatively low complicity timing metrical capacity, with an indoor VLC channel with accuracy Signal/Noise Ratios (SNR) synchronisation of as low as 4 dB.

## 2. LITERATURE REVIEW

DL's treatment for the Deep Nerve Network as a 'black box' was analysed by YUwen YANG in 2019 and the linkages between its inputs and outputs as alternative means of using it in its physical layer. The feed forward network, known as the shallow neural network, is able to approximate any continuous function defined on compact sets. It has been shown to be rigorously in the universal approximation theorem. The DNN is stronger than the shallow neural network because of hidden neurons and layers.

**K. Karra, 2017**, analysed the development of many wireless approaches based on DNNs, such as beam forming, CSI feedback, modulation detection, encoding and decrypting channel, channel estimation and detection. In DNM systems of DNM multiplexing for orthogonal frequency division (OFDM) systems and frequency selective channel systems, especially for imperfections and systems non-linearities the symbol detection algorithm and the joint channel estimate are shown to be above the usual MMSE estimators.

**Fang et.al, 2013**, said that this has a better overhead reduction and enhanced tolerance against laser phase noise, Polarization, chromatic mode dispersion, and noise level. This research work considered only time domain based CE, which is not much suitable for frequency domain CE.

**Qian, 2018**, It has best channel frequency response MSE and BER performance than the LS-CE method, it measured BER, and MSE. This paper didn't present any block diagram on proposed methodology. Hence, the researchers do not easily understand proposed work.

**Savaux, 2015**, The complexity of the system reduced using a low-rank approximation method in the proposed technique, measured BER. This method increased the BER which degraded the system performance.

**Nhan, 2018**, This method achieved less BER. Hence, that method improved significant gain, measured BER, and Peak to Average Power Ratio (PAPR). The performance of the system was affected by the phase noise when fibre nonlinear signals were degraded.

### 3. PROPOSED METHOD

#### OFDM Communication system

The relevant ratings and concepts followed by the channel assessment of conventional receivers are presented for the first time in the physical layer of the lower OFDM system.

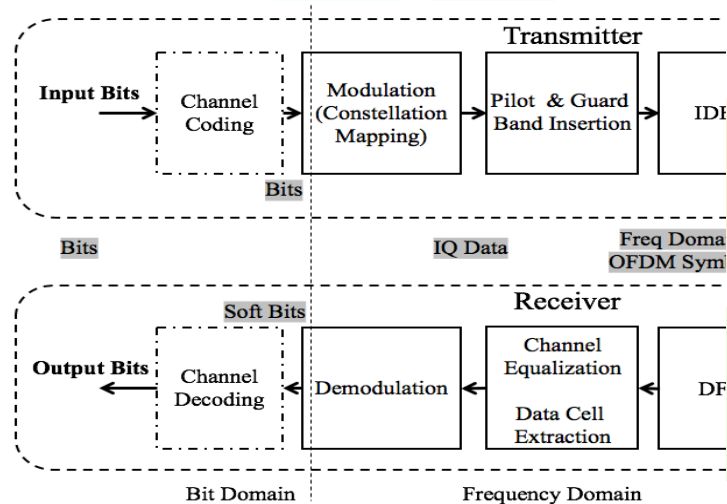
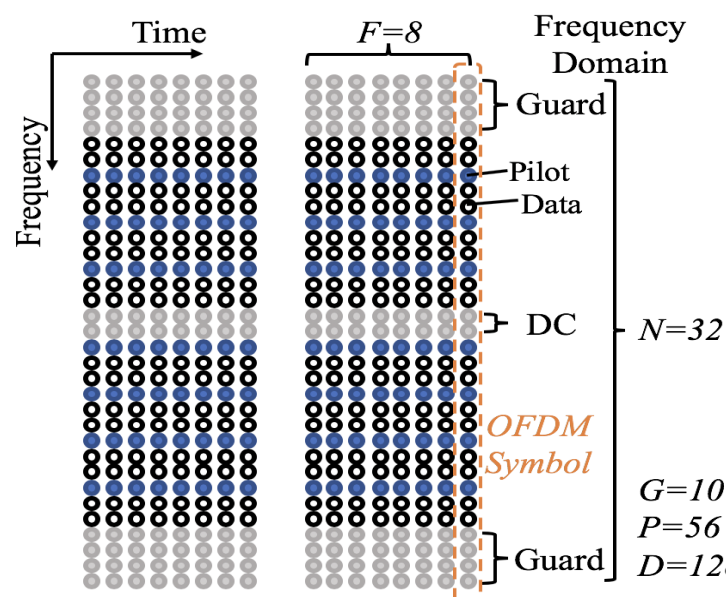


Fig. 2. Physical layer of OFDM system



#### A. Physical Layer

The PHY system block for the OFDM system appears in Figure 2. The encoding of a channel is used first in the input bits  $b \sim \{\pm 1\}$  of the transmitter for the detection and/or correction of an error. In addition to the IQ level of the constellation, the coded bits have been transformed into complex IQ and in-phase data. The X will also be converted into the OFDM time domain, X symbol, via an N-Point IDFT and parallel serial (P/S), when you place the pilots and store the bands in your IQ data. The OFDM frequency domain X symbol will be created. Then at the end of CP, the x section is prepared with x to create the full xcp OFDM time domain symbol, as illustrated in Fig. 3.

Fig 3: Exemplary Slot and Waveform of the OFDM coherence

The xcp signal of the baseband is then transmitted via the RF front end over the air and upgraded to RF. The radio signal is transmitted through the wireless channel and samples are chosen and turned to IQ as a basic band from the receiver front.

#### 3.1 Frame Synchronization in a Pilot-Assisted Optical OFDM System

The preamble/header and payload are usually used to transmit OFDM signal. The categorising approach in OFDM thus builds on the proportion of the signal that is transmitted used to estimate the recipient's symbolic timing compensation. The two large categories of blind and preambular technologies are called [5]. The blind techniques benefit from synchronised OFDM payload's unique features. In order to synchronize the receiver, the blind [9] technique for instance uses the symmetry of the time domain of ACO-OFDM. However, the techniques used in the preamble include the use in the frequency or time domain of the predefined synchronization sequence. A preamble method in [5] uses synchronization of a sign pattern to reduce the computational complexity of O-OFDM for a time domain sequence.

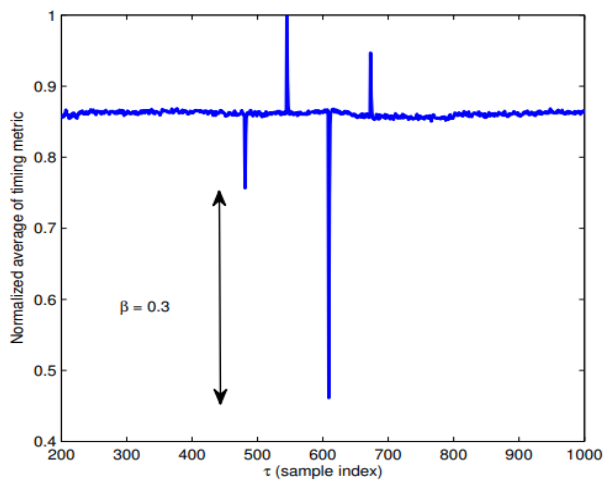


Figure 4. Plot of normalized average of the proposed timing metric (4) for a PA ACO-OFDM with  $N = 256$ ,  $U = 5$ ,  $cp = N/8$ , signal-to-noise ratio (SNR) = 10 dB, and 4-quadrature amplitude modulation (QAM).

The average time metric for a PA-ACO-OFDM is shown in Figure 4. The pilot's beginning symbol is the minimum measuring time. If the pilot symbol is matched by a detection window, the average minimum metric is equal to zero. Although this value is inaccessible because of the effects on the pilot signal of the noise and indoor VLC channel, the proposed PA Frame Timing synchronisation metric still leads to a relative difference between the value at the beginning of a pilot symbol and other points in a frame.

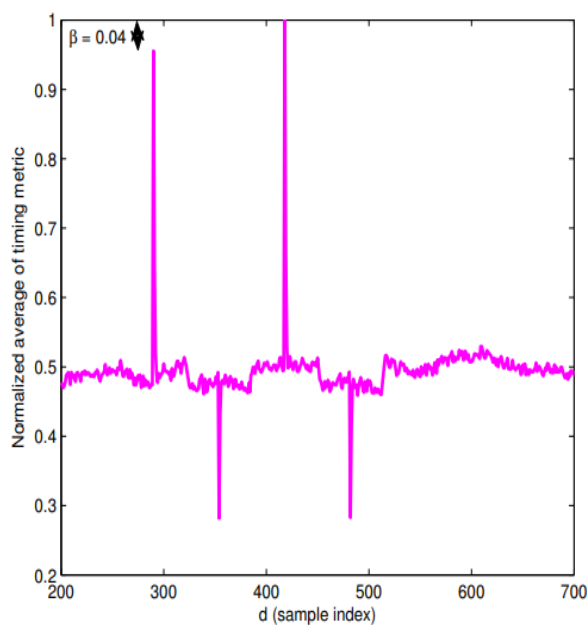


Figure 5. Plot of normalized average of the modified Park's timing metric (6) for an ACO-OFDM system with  $N = 256$ ,  $U = 5$ ,  $cp = N/8$ , SNR = 10 dB, and 4-QAM.

The standard average time metric in cyclical prefix lengths  $N/8$  of the modified park in ACO-OFDM is shown in Figure 5. The right position of the symbol of training is the maximum point of the average time. Let  $\beta = |\beta_P - \beta_2|$  where  $\beta_P$  is the main peak, and  $\beta_2$  the second peak, to quantify the difference between the principle peak and the next peak. On the basis of a training symbol as outlined and the product operation quantity used in the time metric, it is the main and second corresponding peaks with a cyclic prefix of a length greater than or near  $N/8$ .

#### 4. RESULTS AND DISCUSSION

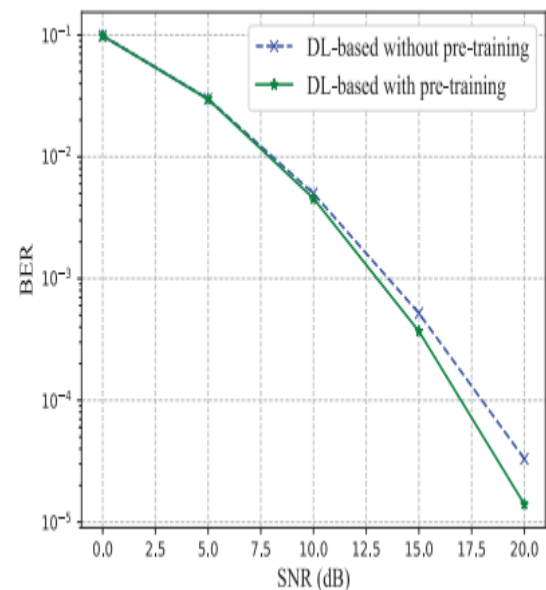


FIGURE 6. Comparison of performance between DL-based pre-training estimators.

The performance of pretraining DL estimators in which  $N_b = 12$  and  $L = 3$  are compared and shown in Fig. 6. The performance improvement of BER is seen as SNR increases. Pre-training. However, this improvement is insignificant if the SNR is below 10 dB.



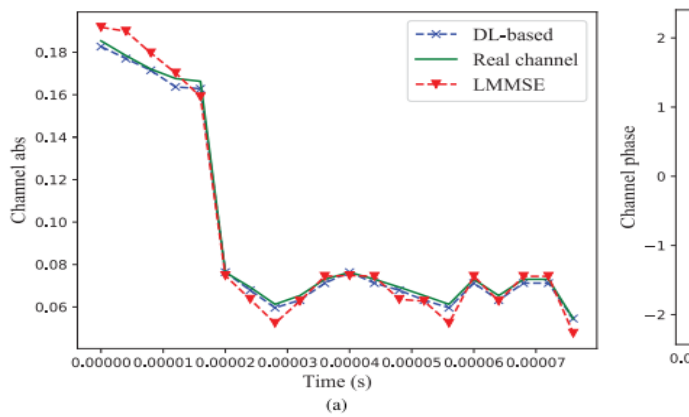


FIGURE 7. Amplitude (a) and phase (b) tracking performance with DL and LMMSE estimators. (a) Tracking of the amplitude. (b) tracking phase.

The proposed DL estimator can be used on doubly selective general channels. This is a special case where the path number is equivalent to 1. Selective time is the time channel. Figure 7 shows the DL and LMMSE channel tracking where the snr is set by 20 dB and Nb by 12. The channel is set by 20 dB.

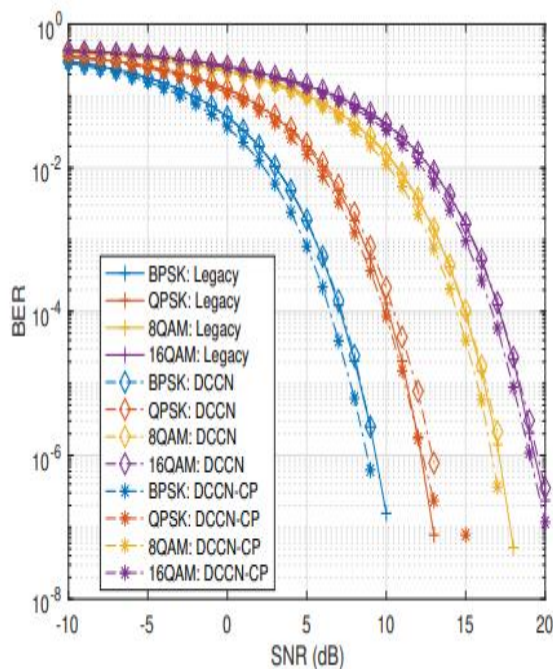


Fig. 8. DCCN OFDM vs. SNR BER and legacy receiver, in AWGN with long CP.

The BER of our basic receiver and legacy OFDM receiver with BPSK, QPSK, 8QAM and 16QAM modularity are listed in Fig. 10 on AWGN channels with SNR from 0.1 to 10 dB where long CP are considered for DCCN-CP.

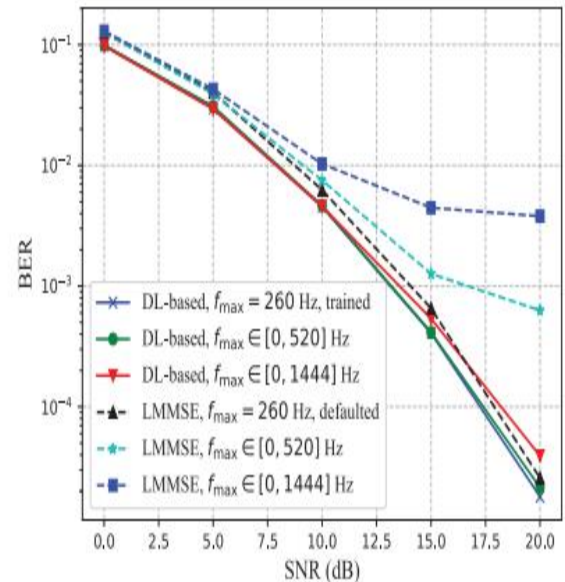


FIGURE 9. The DL-based estimation BER performance and random frequency LMMSE algorithms.

As shown at Fig. 9, the LMMSE estimator BER performance degrades if fmax is randomly variable and SNR degrades. The performance losses caused by the fmax reach difference of 5dB and 9 dB in fmax [0.520] Hz and fmax [0.1444] Hz respectively, especially when the SNR is equivalent to 20dB.

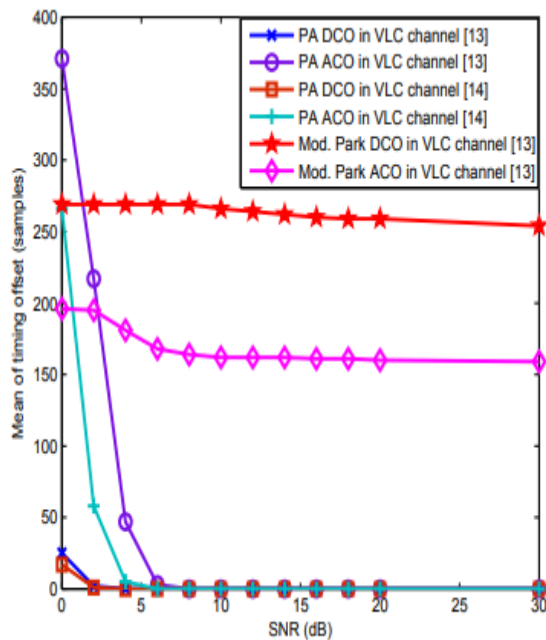


Figure 10. Mean of the timing offset in DCO-OFDM and ACO-OFDM using 1000 frames with  $N = 256$ ,  $U = 5$ ,  $cp = N/16$ , and 4-QAM.

The mean of timing offset for different SNR levels is shown in Figure 10 for DCO-OFDM and ACO-OFDM. In this work a frame time will be estimated precisely if at the start of a pilot or training symbol the timing metric gives its main peak without any tolerance margin.

## CONCLUSION

Deep Complex's DCCN, end-to-end OFDM receivers, was proposed in this paper to recover uncoded bits from synchronised OFDM time domain signals. Instead of treating the real and imaginary components of sampling IQ as a segmented stream, DCCN follows the rules for multiplication in complex fields, with the intention, of replacing DFT/IDFT with OFDM systems and using a cyclic preset redundancy on the OFDM waveform. The Pilot Time Domain pattern strengthens the method by applying a cyclic prefix length to the time metric, so it gives the main peak at the start of the Pilot Symbol. Results show that the proposed time metric can be used for exact framing synchronization in indoor VLC channels if SNR  $\geq 4$  dB and SNR  $\geq 8$  dB are present on DCO-OFDM and ACO-OFDM. However, if the SNR declines, the algorithm can synchronize the frame accurately.

## REFERENCES

- [1] T. Wang, C. Wen, H. Wang, F. Gao, T. Jiang, and S. Jin, "Deep learning for wireless physical layer: Opportunities and challenges," *China Communications*, vol. 14, no. 11, pp. 92–111, Nov 2017.
- [2] Q. Mao, F. Hu, and Q. Hao, "Deep learning for intelligent wireless networks: A comprehensive survey," *IEEE Communications Surveys Tutorials*, pp. 1–1, 2018.
- [3] D. Gunduz, P. de Kerret, N. D. Sidiropoulos, D. Gesbert, C. R. Murthy, and M. van der Schaar, "Machine learning in the air," *IEEE Journal on Selected Areas in Communications*, vol. 37, no. 10, pp. 2184–2199, 2019.
- [4] T. J. O'Shea, J. Corgan, and T. C. Clancy, "Convolutional radio modulation recognition networks," in *Engineering Applications of Neural Networks*, C. Jayne and L. Iliadis, Eds. Cham: Springer International Publishing, 2016, pp. 213–226.
- [5] T. J. O'Shea, L. Pemula, D. Batra, and T. C. Clancy, "Radio transformer networks: Attention models for learning to synchronize in wireless systems," in *2016 50th Asilomar Conference on Signals, Systems and Computers*, Nov 2016, pp. 662–666.
- [6] D. K. Borah and B. T. Hart, "Frequency-selective fading channel estimation with a polynomial time-varying channel model," *IEEE Trans. Commun.*, vol. 47, no. 6, pp. 862–873, Jun. 1999.
- [7] M. Martone, "Wavelet-based separating kernels for array processing of cellular DS/CDMA signals in fast fading," *IEEE Trans. Commun.*, vol. 48, no. 6, pp. 979–995, Jun. 2000.
- [8] W. Cheng, H. Zhang, L. Liang, H. Jing, and Z. Li, "Orbitalangular-momentum embedded massive MIMO: Achieving multiplicative spectrum-efficiency for mmWave communications," *IEEE Access*, vol. 6, pp. 2732–2745, Dec. 2018.
- [9] J. K. Tugnait, S. He, and H. Kim, "Doubly selective channel estimation using exponential basis models and subblock tracking," *IEEE Trans. Signal Process.*, vol. 58, no. 3, pp. 1275–1289, Mar. 2010.
- [10] J. T. Dias, R. C. de Lamare, and Y. V. Zakharov, "BEM-based channel estimation for 5G multicarrier systems," in *Proc. 22nd Int. ITG Workshop Smart Antennas (WSA)*, Bochum, Germany, Mar. 2018, pp. 1–5.